The Effect of the Particle Size on the Fundamental Vibrations of the [CO_3^{2-}] Anion in Calcite

Petra Kristova*[1], Laurence J. Hopkinson[2] and Ken J. Rutt[1]

[1] School of Pharmacy and Biomolecular Sciences,

University of Brighton.

Huxley Building, Lewes Road, Brighton.BN2 4GJ.

United Kingdom.

Tel: +44 (0)1273 642065, Fax: +44 (0)1273 642285, e.mail: p.kristova@brighton.ac.uk

Tel: +44 (0)1273 642076, Fax: +44 (0)1273 642285, e.mail: k.j.rutt@brighton.ac.uk

[2] School of the Environment and Technology,

University of Brighton

Cockcroft Building, Lewes Road, Brighton.BN2 4GJ.

United Kingdom.

Tel: +44 (0)1273 642239, Fax: +44 (0)1273 642285, e.mail: l.hopkinson@brighton.ac.uk

Key words: particle size effect, calcite, optical properties, spectroscopy

Abstract

This study examines the effects of particle sizes between 3-121μm on the fundamental vibrations of the [CO_3^{2-}] anion in calcite [$CaCO_3$] as analyzed by total attenuated reflectance infrared spectroscopy (ATR-IR) and Raman spectroscopy (RS). The ATR-IR absorbance intensity ratios of the [v_4/v_3] [$712cm^{-1}/1393cm^{-1}$], [v_4/v_2] [$712cm^{-1}/871cm^{-1}$] and [v_2/v_3] [$871cm^{-1}/1393cm^{-1}$] share the same profile for grain size fractions 121μm through to 42μm mode. Between 42 and 3μm mode the three ratios sharply decline in a systematic manner, consistent with a non-uniform decrease in spectral contrast of the [CO_3^{2-}] internal modes. Raman intensity increased with decreasing particle size from 121μm until 19μm mode particle size fraction thereafter decreasing sharply. The [v_4/v_3], [v_1/v_3] and [v_4/v_1] intensity ratios normalised against the corresponding intensity ratio of the 121μm particle size fraction, indicate that the [v_4/v_3] ratio changes by 22%. Both ATR-IR and Raman indicate two critical points in internal mode behaviour of the Raman and infrared active v_4 and v_3 internal modes, the first, at between 42-59μm size range and the second between 19 and 5μm. Results are interpreted in terms of specular to volume (diffuse) coherent transitions of internal modes and with further grain refinement internal mode specific optically thick to thin transitions.

1. Introduction

Calcite forms rhombohedral (trigonal) crystal units with a unit cell containing two carbonate ions pointing in opposite direction. The [CO_3^{2-}] anion in calcite [$CaCO_3$] shows four internal modes, i.e. the v_1 symmetrical stretch (Raman active), the v_2 out-of-plane bend (infrared-active), the v_3 anti-symmetric stretching and the v_4 in-plane bending mode. The latter two are infrared and Raman active.[1] It is well established that the positions of these infrared and Raman bands measured from a single uniaxial calcite crystal are dependent on whether the measurement is taken transversely or longitudinally relative to the optical axis of the crystal.[1-2] Conversely measurements from powdered samples are assumed to minimize crystal axis dependency, i.e. emissivity of ordinary and extraordinary rays.[2] Hence measurements taken from powders do not provide a precise representation of either the transverse or longitudinal measurement but fall somewhere between the two.[1]

Spectral intensities (infrared absorption and Raman intensity) are generally considered proportional to concentration by Boguer-Lambert-Beer Law or by other mathematical formulae derived from the fundamental law of quantitative spectroscopy.[3-6] However infrared spectra acquired from powdered calcite and other mineral species are known to undergo changes as a function of particle grain size.[2,7-9] The effect of particle size on the spectral resolution of the fundamental vibrations of the [CO_3^{2-}] anion in calcite were identified in infrared emission studies and have been divided into three classes of behavior.[2,10-11] Type 1 behavior shows a decrease in spectral contrast with decreasing particle size. Type 2 shows an initial decrease in spectral contrast with decreasing particle size upon reaching a critical particle size, at which point the original emissivity trough reverses into a peak (and *vice versa* for reflectance) with decreasing particle size. Type 3

behavior involves an increase in spectral contrast with decreasing particle size.[10] The calcite v_3 anti-symmetric stretching mode shows type 1 behavior, whereas the [CO_3^{2-}] bending modes ν_2 and ν_4 show type 2 behavior.[2,8] One of the main conceptual interpretations arising from these differing type behaviors is that two competing factors contribute to the observed spectral response, i.e. part of the spectral signal comes from the specular (surface-scattered) component and part from volume of sample grains (diffuse) component, the relative contribution of the two components to the observed spectral response evolving as a function of grain refinement.[11]

The Fresnel equation has been employed to predict type behavior based on the refractive index of calcite[2,12-13] which contains a real (*n)* and imaginary *(k)* component, where (*n*) indicates refractive index and (*k*) correlates to absorption i.e. the amount of absorption loss when the electromagnetic wave propagates through the material.[3] Both *(n)* and (*k)* are dependent on the wavelength. The critical diameter for a transition in optical properties is related to the absorption coefficient (α) and is proportional to wavelength (λ) and (*k*) defined as[2,13]:

$$\alpha = 4\pi k/\lambda \qquad [1]$$

At the same time the absorption coefficient corresponding to transmittance (*T*) is given by[11,13]:

$$T = e^{-\alpha d} \qquad [2]$$

where *d* is the mean photon path length through grains. In general when material possesses a sufficiently large *k* and α*d* is >> *1* it means that the surface reflection may also be large and the material is referred to as optically thick.[13] Optically thin materials

possess sufficiently small *(k)* values that αd is ≤ 1. Consequently volume (diffuse) scattering dominates. Accordingly the reflectance spectrum is then qualitatively similar to the transmittance spectrum. With respect to the v_3 anti-symmetric stretching mode for calcite, the optically thick-thin transition resides in the *ca.* 63μm (and smaller) particle size fraction.[2]

The effect of powder particle sizes on IR spectral measurements has also been explained in terms of Mie theory, which relates the refractive index of a particle relative to the surrounding medium and a size parameter.[14] The theory strictly applies to spherical particles that are small in size in comparison with the wavelength of incident light.[12,14-16] However particle size reduction often imparts change in particle shapes, the effect of which on IR spectra has been discussed in very few studies and primarily in the context of inhomogeneity in powdered samples.[17-18] However it has been shown that the reflectance spectra of optically uniaxial (α-Fe_2O_3) particles, measured as bulk material pressed in pellets, changes with the axial ratios of the particles.[18] Furthermore physical compression, packing and porosity of powdered materials also play important roles in shaping the spectral response.[8,16,19]

By comparison with infrared studies, particle size effects on Raman spectra are poorly documented. Specifically how the type-behaviors of [CO_3^{2-}] internal modes in calcite as described by infrared spectroscopy find expression in relation to particle size effects detectable in Raman spectroscopy, although available evidence suggests that the absolute intensity of the [CO_3^{2-}] internal modes of carbonate minerals do vary as a function of powder particle size ranges.[6,20] To this end this study examines the effects of powder particle size ranges and the optically thick to thin transition on the fundamental

vibrations of the $[CO]_3^{2-}$ anion in calcite by attenuated total reflectance mid-infrared (ATR-IR) and Raman spectroscopy (RS).

2. Materials and methods

Large (*ca.* 7cm longest dimension) transparent euhedral calcite crystals (Iceland spar) were manually crushed and dry-milled using a ZrO_2 (Fritsch, planetary monomill) ball mill operating at 250rpm for 3 minutes. Six sieved fractions were then washed with absolute alcohol to remove any clinging fines. The two finest grain fractions were prepared as follows. The supernatant from washing the samples was filtered and the obtained powder was split into two parts, one of which underwent additional milling under water at 400rpm for 20minutes, collectively yielding a total of eight separate particle size fractions.

Particle size analysis was performed by laser diffraction using a Malvern Mastersizer 2000 particle size analyzer, equipped with single lens detection and dual wavelength measurement by blue and red light. Samples were measured (over range 0.02-2000μm) suspended in water using a Malvern Hydro 2000G dispersion unit. The ground calcite samples were analyzed without addition of any surface active agent and without employing an ultrasonic device. Particle sizes and shapes were ascertained by scanning electron microscopy (SEM) (Carl Zeiss, EVO LS15) utilizing a secondary scattering technique. Samples were mounted on specimen stubs and coated with 4nm platinum (Quorum, Q150T ES sputter coater).

Mid-infrared spectroscopic measurements were performed using a Perkin Elmer, Spectrum 65 spectrometer, fitted with an attenuated total reflectance (ATR) accessory employing a ZnSe crystal. Measurements through the ATR accessory require good contact between the sample and the ZnSe crystal. This was achieved by uniform light

manual compaction. The samples were measured in the spectral range 4000-600cm^{-1} at a resolution of 4cm^{-1}. Each spectrum was collected from 16 scans and repeated six times on different subsamples to assure representative spectral information. Raman analyses were conducted using a Perkin Elmer Raman Identicheck fitted with a 785nm diode laser and with a CCD detector, thermoelectrically cooled to -50°C. The measurements were acquired utilizing a fiber optic probe (spot size of 100μm at a working distance of 7.5mm) at 100mV laser power. The bulk samples of powdered calcite were measured placed in brass holders and covered by a silica-glass slide to ensure a smooth surface interface. Raman spectra were taken in the spectral range 2000-300cm^{-1} at a resolution of 2cm^{-1}. Each spectrum was collected from 8 scans for 2 seconds and repeated six times on different randomly selected subsamples to assure representative spectral information and that sample preparation did not result in the polymorphic transition of calcite to aragonite.[21] The later mineral would show Raman active bands[22] at 704, 1462, 1574cm^{-1} for which no evidence was found in any sample. The limit of detection for the Raman system operating on pressed powders is *ca.* 2% or better.[6] All analyses were conducted at 25°C, at atmospheric pressure at the University of Brighton U.K.

3. Results

3.1 Particle size and shape analyses

The mode sizes of grain fractions of the powders were measured as 3µm, 5µm, 19µm, 24µm, 42µm, 59µm, 83µm and 121µm by laser diffraction (Table 1). Grain size fractions washed prior to analysis (≥19µm modal) showed mono-modal distributions. The finest fractions (3 and 5µm mode) showed poly-disperse profile distributions (Figure 1). SEM analysis indicates that calcite from the largest grain size fraction (121µm mode) consists of well-cleaved rhombs which show locally intense irregular micro-fracturing, interspersed with finer grained anhedral particles ranging in size from a few micrometers to <0.5µm (Figure 2a). With increasing particle size reduction rhombs become scarcer, show progressively more evidence of micro-fracturing and become more equant (Figure 2b,c). Mode size 24 and 19µm samples contain many irregular fragments with few remaining tabular crystals which range in size from *ca.* 5 to 30µm (Figure 2d,e). The finest fractions are characterized by particles which are largely devoid of planar surfaces. Particle sizes range from *ca.* 6µm to *ca.* 100nm and are arranged in agglomerates. The additional very fine particles (<0.4µm) were not resolved by laser diffraction (Figure 2f).

particle size fraction [µm]	mode size [µm] by laser diffraction
106-90	121
90-75	83
75-64	59
64-45	42

below 45	24
below 38	19
fines 1	5
fines 2	3

Table 1: Calcite particle size fractions and their mode size, measured by laser diffraction.

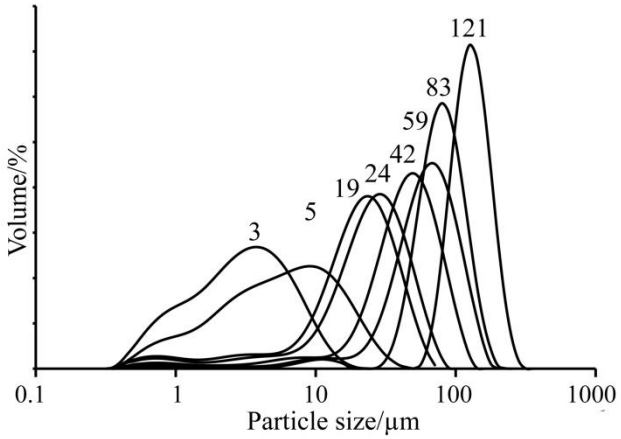

Figure 1: Particle size analysis of prepared calcite fractions measured by laser diffraction. Numbers above individual size distributions indicate mode sizes (μm) of the fractions.

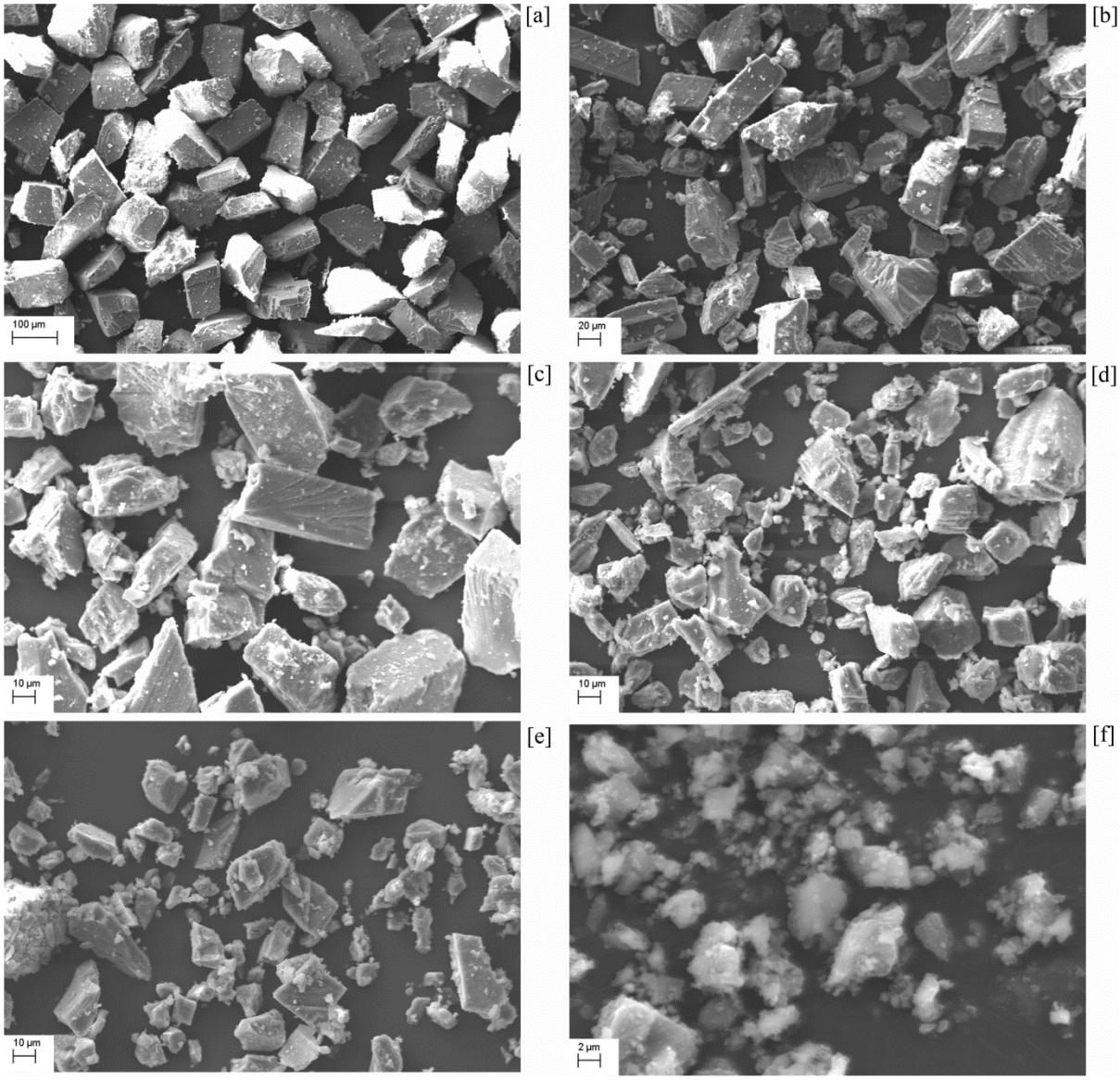

Figure 2: Scanning electron microscope images of calcite particles. (a) mode size 121µm (b) mode size 59µm (c) mode size 42µm (d) 24µm (e) mode size 19µm (f) mode size 3µm.

3.2 Mid-infrared spectroscopy

The ATR-IR spectrum of Iceland spar (121µm powder) is shown in Figure 3. The spectrum shows the dominant peak at 1393cm^{-1} assigned to [CO_3^{2-}] ν_3 asymmetric stretch. The ν_3 peak is asymmetric with a shoulder at 1403cm^{-1}. The out-of-plane bending

ν_2 band which is the second highest intensity band occurs at 871cm^{-1} with a subordinate weak peak at 847cm^{-1}. The in-plane bending mode ν_4 occurs at 712cm^{-1} wavenumbers. The spectrum also shows weak bands at 1795, 2512, 2874 and 2980cm^{-1} which are assigned to calcite combination bands and harmonic oscillatory bands.[23-24] The infrared forbidden ν_1 symmetric stretch occurs as a very weak peak at 1088cm^{-1} (Figure 3).

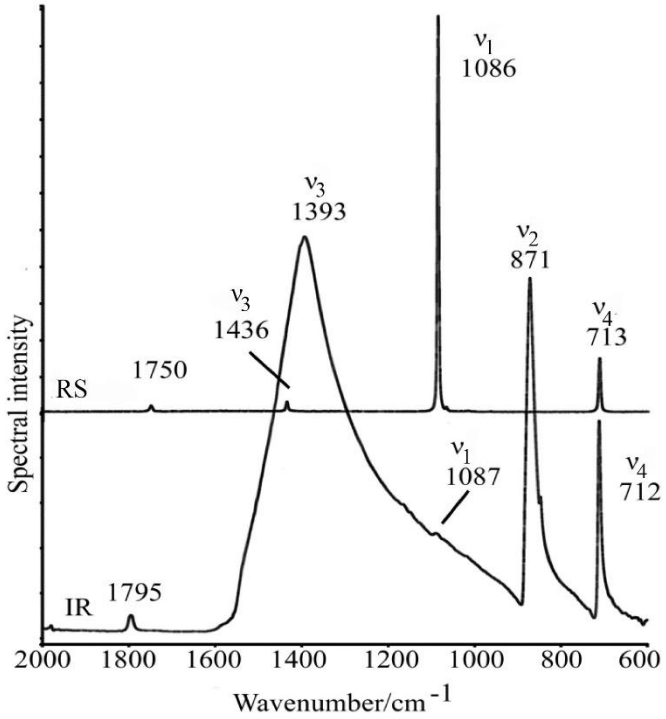

Figure 3: The ATR-IR and Raman spectra of powdered (121µm mode particle size) calcite. Note, the intensity of the ν_3 asymmetric stretch and ν_4 in-plane bend vibrations of the carbonate anion in Raman spectra of calcite are invariably described as very weak and weak respectively.[22] Conversely ν_3 is the strongest feature in the infrared spectrum and ν_4 is strong.[1]

Figure 4 shows the absorbance intensity ratios of the bending and stretching modes of [ν_4/ν_3] [712cm^{-1}/1393cm^{-1}], [ν_4/ν_2] [712cm^{-1}/871cm^{-1}] and [ν_2/ν_3] [871cm^{-1}/1393cm^{-1}] plotted against mode grain size fractions. The calculated ratios share the same profile for grain size fractions 121µm through to 42µm mode. Between 42 and 3µm mode the three

ratios sharply decline in a systematic manner from 0.51 to 0.26 [ν_4/ν_3], 0.64 to 0.37 [ν_4/ν_2] and 0.94 to 0.70 [ν_2/ν_3], consistent with a non-uniform decrease in spectral contrast of the [CO_3^{2-}] internal modes. The strength of ν_4 absorbance decreases preferentially relative to ν_2 and ν_3. While ν_2 absorbance strength also decreases preferentially relative to ν_3 absorbance.

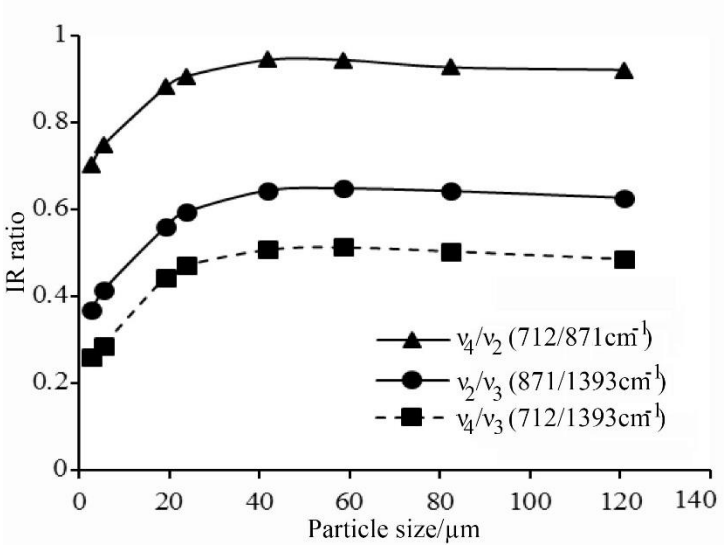

Figure 4: Calcite IR-ATR ratios of ν_4/ν_2 ($712cm^{-1}/871cm^{-1}$), ν_2/ν_3 ($871cm^{-1}/1393cm^{-1}$) and ν_4/ν_3 ($712cm^{-1}/1393cm^{-1}$) plotted against grain size (modal sizes in microns).

3.3 Raman spectroscopy

The Raman internal modes of calcite were measured at (ν_1) $1086cm^{-1}$ (very strong), (ν_4) $713cm^{-1}$ (weak) and (ν_3) $1436cm^{-1}$ (very weak) (Figure 3). The Raman intensity of the bands increased with decreasing particle size from 121μm until 24μm mode particle size fraction (Figure 5a). Below this size the absolute Raman intensity of all measured bands progressively decreased with decreasing particle size. Figure 5b shows the [ν_4/ν_3], [ν_1/ν_3] and [ν_4/ν_1] intensity ratios normalised against the corresponding intensity ratio of the 121μm particle size fraction, with change expressed as a percentage. The [ν_4/ν_3] the ratio

changes by 22% (ratio ranges from 4.6 to 5.9). The ratio increases with decreasing particle size over the range 121-59μm grain size. Thereafter the ratio decreases with decreasing particle size with a possible change in rate of decrease of the ratio between 5 and 3μm. The average relative standard deviation was calculated at 4%. A similar trend is observed for the [ν_1/ν_3] ratio. A significantly smaller change in the [ν_4/ν_1] (*ca.* 5%) is also evident with the maximum [ν_1/ν_3] ratio obtained from the 42μm mode sample.

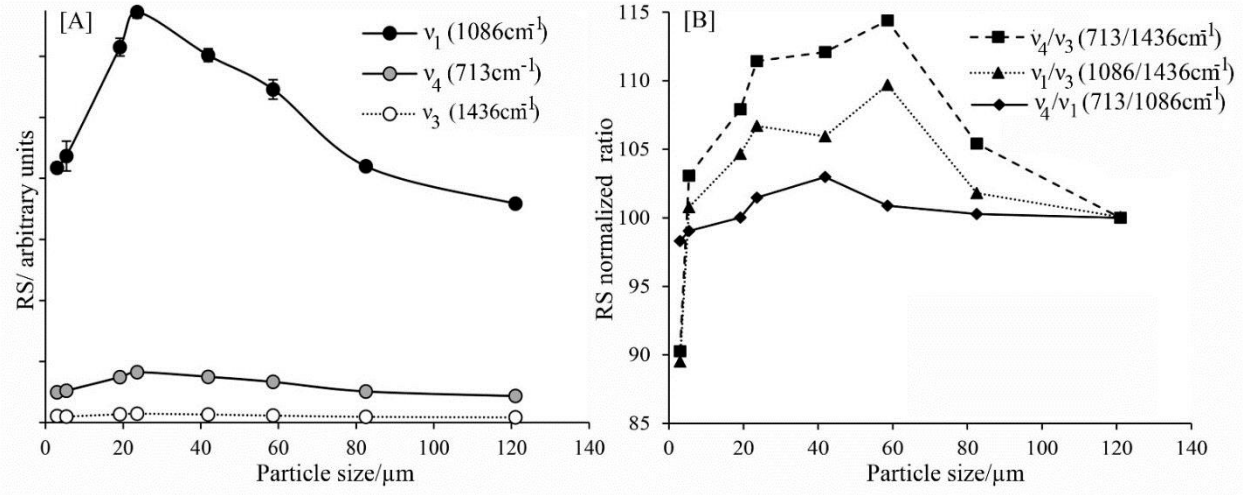

Figure 5: [A] Raman intensity (peak heights in absolute values) plotted against grain size (modal sizes in microns). [B] Raman ratios ν_4/ν_3 (713cm^{-1}/1436cm^{-1}), ν_1/ν_3 (1086cm^{-1}/1436cm^{-1}) and ν_4/ν_1 (713cm^{-1}/1086cm^{-1}) normalized to 100 at 121μm mode particle size fraction and plotted against particle size.

4. Discussion

SEM findings indicate the gradational change in dominance of characteristic shapes and three critical size interval ranges. Namely coarse rhombic fragment dominated powder (121-59μm) which undergoes progressive transition to intensely micro-fractured equant-shaped grains (*ca.* 59-42μm to 19μm), which are then progressively transformed (≤ 5μm) to sub-micron shards arranged in ramified aggregates. The progressive loss of planar surfaces accompanying grain size reduction with associated increase in micro-fracturing of particles would collectively serve to increase the overall amount of volume scattering (i.e. energy propagation in the matrix after initial boundary interaction relative to specular reflectance), through progressively increasing numbers of inter-particle multiple and intra-particle (internal) scattering events. Because of the large value of *k* associated with the internal modes[2] energy absorbance by the grains would undergo a concomitant increase. The Raman spectra show an overall increase in intensity with grain size reduction over the *ca.* 121μm to 42μm particle size range, consistent with some previous findings on the relationship between constituent particle size in powders and Raman intensity.[20] A possible explanation for the phenomenon may reside in porosity reduction with progressive closer packing of finer grained particles, serving to enhance the intensity of the Raman signal.

Figure 6 shows the [ν_4/ν_3] ratio acquired by ATR-IR plotted against the corresponding ratio acquired by Raman. Both sets of data are normalized to 100% with respect to the 121μm grain size fraction. The disposition of the data is divisible into three sections, marked intervals A (121-59μm), B (59-5μm) and C (5-3μm) respectively. The IR and Raman results qualitatively correlate with the morphological sub-divisions defined by

SEM. The values of normalized change in the [ν_4/ν_3] ratios divided by change in particle size was used to calculate rates of incline and decline for the Raman and ATR-IR [ν_4/ν_3]. During interval A the Raman and ATR-IR [ν_4/ν_3] ratios increase relative to the said ratio for the 121µm grain size fraction. The incline is 0.23 and 0.09 for RS and ATR-IR respectively. Interval B shows rates of decline of 0.21 (RS) and 0.86 (ATR-IR). Interval C shows rates of decline of 5.57 and 2.87 for RS and ATR-IR respectively (Table 2).

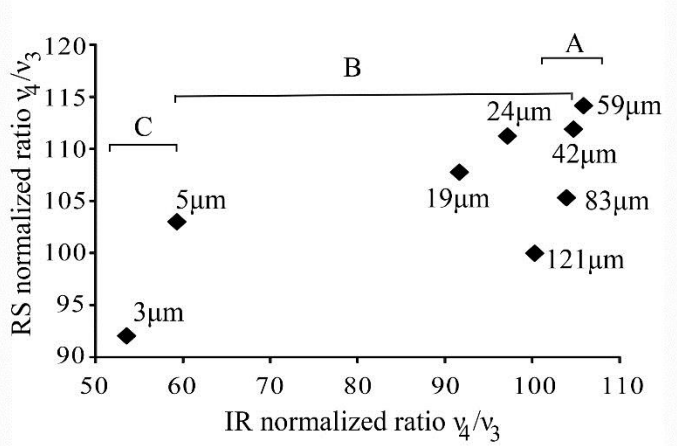

Figure 6: Ratios [ν_4/ν_3] yielded from IR-ATR ($712cm^{-1}/1393cm^{-1}$) plotted against ratios of RS ($713cm^{-1}/1436cm^{-1}$).

interval	size [µm]	size change [µm]	IR (%) ν_4/ν_3	IR change	IR rate	RS (%) ν_4/ν_3	RS change	RS rate
A1	121		100.00			100.00		
A2	83	38.00	103.63	-3.63	-0.10	105.42	-5.42	-0.14
A3	59	24.00	105.58	-1.95	-0.08	114.40	-8.98	-0.37
total (A1- A3)		62.00		-5.58	-0.09		-14.40	-0.23
B1	59		105.58			114.40		
B2	42	17.00	104.43	1.15	0.07	112.11	2.29	0.13
B3	24	18.00	96.89	7.54	0.42	111.44	0.67	0.04
B4	19	5.00	91.40	5.49	1.10	107.91	3.52	0.70
B5	5	14.00	59.15	45.28	3.23	103.07	4.84	0.35
total (B1-B5)		54.00		46.43	0.86		11.33	0.21
C1	5		59.15			103.07		
C2	3	2.00	53.42	5.74	2.87	91.94	11.13	5.57

total (C1-C2)	2.00		5.74	2.87		11.13	5.57

Table 2: Comparison of IR and Raman rates in intervals A, B and C (see Figure 6).

ATR-IR and Raman show that the 121μm-normalised [ν_4/ν_3] ratio increases in the 121-59μm particle size range with decreasing particle size (Figure 6). The ν_4 bending mode possesses a lower absorption coefficient than ν_3 anti-symmetric stretch because the value of k is smaller and because ν_4 is located at a higher wavelength value (lower wavenumber) than ν_3.[2] Consequently the observed change in the 121μm-normalised [ν_4/ν_3] ratio may arise because ν_4 would preferentially increase relative to ν_3 because of greater internal scattering (and therefore absorption) of ν_4 relative to ν_3 accompanying particle size reduction within interval A. Accepting this it follows that the RS data which shows a similar 121μm-normalised [ν_4/ν_3] trend in the 121-59μm size interval to ATR-IR (Figure 6) may similarly arise from greater internal scattering of ν_4 relative to ν_3 accompanying particle size reduction within interval A. As for any given fixed particle size the relative contribution of the specular and diffuse components to spectral contrast is singular to the specific internal mode. It is also apparent that the rate of change of the 121μm-normalised [ν_4/ν_3] ratio is discernably more marked in Raman data than corresponding ATR-IR data (Figure 6). One possible reason for this disparity relates to experimental conditions. Specifically the porosity in an ATR-IR analysis can be expected to be significantly lower than in the corresponding Raman analysis because the former technique requires the application of a greater contact pressure upon the powder during data acquisition.

ATR-IR and RS data indicate that the 121μm-normalised [ν_4/ν_3] ratios undergo pronounced reduction which commences in the 59-42μm region through to the 5μm size fraction (Figure 6). It is of note that infrared (thermal) emissivity studies of calcite

powders identify the optically thick-thin transition as residing in the *ca.* 63μm (and smaller) particle size fraction.[2] Hence ATR-IR and Raman data appear to register the same phenomenon. In other words the turn-around in the 121μm-normalised [v_4/v_3] ratio within domain B registers the abrupt transition from the dominance of surface to volume scattering by the v_3 internal mode, registered in the 121μm-normalised [v_4/v_3] ratio at some value between 59μm and 42μm. The 121μm-normalised [v_4/v_3] ratio thereafter declines with decreasing grain size. It is evident that ATR-IR data shows a markedly higher rate of decline in interval B (59-5μm) than corresponding Raman data (Table 2). One possible explanation is a preferential decrease in the dipole moment relative to the polarizability of the molecule.

Raman intensity decreases steeply in powders less than 24μm particle size (Figure 5a). Associated with this the Raman [v_4/v_3] [v_1/v_3] [v_4/v_1] (Figure 5a) and ATR-IR [v_4/v_2] [v_2/v_3] and [v_4/v_3] ratios decrease in a systematic manner (Figure 4). Equations [1] and [2] indicate a relationship between particle size and wavelength. Mineral particles may become optically thin when the particle size is equal or smaller than the measured wavelength.[13] The wavelength of the internal modes equate to particle sizes: v_1 = 9μm; v_2 = 11μm; v_3 = 7μm; v_4 = 14μm. The values are intermediate between the 19μm and 5μm modal fraction powders indicating that growing proportions of each powder fraction from 19μm to 5μm to 3μm contain an increasing population of particles which are optically thin with respect to one or more internal modes. A large majority of the 3μm mode powder fraction is optically thin with respect to all internal modes (Figure 1). It is generally accepted that the spectral contrast of internal modes decrease as particle size decreases and that when separated by more than a wavelength particles behave as optically thin incoherent volume-scatterers. Conversely when packed closely together

they scatter coherently as if optically thick surface scattering particles.[8] Hence the progressive degradation of the overall intensity of contrast of all spectral features at <24μm is assigned to increasing volume scattering, the growing proportion of optically thin constituents to the population and, their immediate packing arrangement. Differences in internal mode ratios accompanying this transition remain fixed because relative spectral contrast is singular to the specific internal mode.

5. Conclusions

Raman and ATR-infrared results show systematic changes in internal mode behaviour as expressed by ratios within the size range 121-3μm mode range. In particular the [v_4/v_3] ratio (for which both internal modes are Raman and infrared active) is interpreted to undergo an abrupt transition (between 59 and 42μm size fractions) from specular to coherent diffuse scattering, coincident with loss of crystallographic habit accompanying progressive grain refinement. The v_4 bending mode is interpreted to be strongly volume diffusive across the range of experimental particle sizes examined. Coherent volume scattering is progressively accompanied by incoherent scattering from 19μm through to 3μm modal particle size powders resulting in weakening of spectral contrast. The later samples show abundant agglomerates of sub-micron sized particles. The associated trends in internal mode ratios are assigned to progressively increasing proportions of finer grained fractions crossing of the optical thick-thin transition. Wider implications of this work are important with respect to characterization of fine particles in dusts related to planetary exploration programmes as well as any semiquantitative spectroscopic works using ratios.

Acknowledgements

The University of Brighton is thanked for financial support

References

1. White, W.B. The Carbonate Minerals. The Infrared Spectra of Minerals, Editor Farmer, V.C., Mineralogical Society Monograph 4, London, U.K., 1974
2. Lane, M. Midinfrared Optical Constants of Calcite and Their Relationship to Particle Size Effects in Thermal Emission Spectra of Granular Calcite. J. Geophys. Res. 1999, 104, 14099-14108
3. Griffiths, P.R.; Haseth, J.A. Fourier Transform Infrared Spectrometry, Chemical Analysis, A Series of Monographs on Analytical Chemistry and Its Applications, Series Editor Winefordner, J.D., Wiley, U.K., 2007
4. Sherazi, S.T.H.; Ali, M.; Mahesar, S.A. Application of Fourier-Transform Infrared (FT-IR) Transmission Spectroscopy for the Estimation of Roxithromycin in Pharmaceutical Formulations. Vib. Spectrosc. 2011, 55, 115–118
5. Chen, Z.P.; Li, L.M.; Jin, J.W.; Nordon, A.; Littlejohn, D.; Yang, J.; Zhang, J.; Yu, R.Q. Quantitative Analysis of Powder Mixtures by Raman Spectrometry: the Influence of Particle Size and Its Correction. Anal. Chem. 2012, 84, 4088-4094
6. Kristova, P.; Hopkinson, L.; Rutt, K.; Hazel, H.; Cressey, G. Quantitative Analyses of Powdered Multi-Minerallic Carbonate Aggregates Using a Portable Raman Spectrometer. Am. Mineral. 2013, 98, 401-409
7. Hunt, G.R.; Logan, L.M. Variation of Single Particle Mid-Infrared Emission Spectrum with Particle Size. Appl. Optics 1972, 11, 142-147

8. Salisbury, J.W.; Wald, A. The Role of Volume Scattering in Reducing Spectral Contrast of Reststrahlen Bands in Spectra of Powdered Minerals. Icarus 1992, 96, 121-128
9. Hirsch, H.; Arnold, G. Fourier-Transform Spectroscopy in Remote-Sensing of Solid Planetary Surfaces. Vib. Spectrosc. 1993, 5, 119-123
10. Hunt, G.R.; Vincent, R.K. The Behavior of Spectral Features in the Infrared Emission from Particulate Surfaces of Various Grain Sizes. J. Geophys. Res. 1968, 73, 6039-6046
11. Vincent, R.K.; Hunt, G.R. Infrared Reflectance from Mat Surfaces. Appl. Optics 1968, 7, 53-59
12. Hapke, B. Bidirectional Reflectance Spectroscopy: 1. Theory. J. Geophys. Res.: Solid Earth 1981, 86, 3039–3054
13. Salisbury, J.W.; Hapke, B.; Eastes, J.W. Usefulness of Weak Bands in Midinfrared Remote Sensing of Particulate Planetary Surfaces. J. Geophys. Res. 1987, 92, 702-710
14. Hapke, B. Theory of Reflectance and Emittance Spectroscopy. Cambridge University Press: Cambridge, U.K., 2012
15. Conel, J.E. Infrared Emissivities of Silicates: Experimental Results and a Cloudy Atmosphere Model of Spectral Emission from Condensed Particulate Mediums. J. Geophys. Res. 1969, 74, 1614-1634
16. Hapke, B. Bidirectional Reflectance Spectroscopy 6. Effects of Porosity. Icarus 2008, 195, 918-926
17. Serna, C.J.; Ocafia, M.; Iglesias, J.E. Optical Properties of α-Fe_2O_3 Microcrystals in the Infrared. J. Phys. Part C Solid. 1987, 20, 473-484
18. Pecharroman, C.; Iglesias, J.E. Effect of Particle Shape on IR Reflectance Spectra of

Pressed Powders of Anisotropic Materials. Appl. Spectrosc. 2000, 54, 634-638

19. Salisbury, J.W.; Eastes, J.W. The Effect of Particle Size and Porosity on Spectral Contrast in the Mid-Infrared. Icarus 1985, 64, 586-588
20. Pellow-Jarman, M., Hendra, P.J., and Lehnert, R.J. The Dependence of Raman Signal Intensity on Particle Size for Crystal Powders. Vib. Spectrosc. 1996, 12, 257-261
21. Li, T.; Sui, F.; Li, F.; Cai, Y.; Jin, Z. Effects of Dry Grinding on the Structure and Granularity of Calcite and Its Polymorphic Transformation into Aragonite. Powder Technol. 2014, 254, 338-343
22. Edwards, H.G.M.; Villar, S.E.J.; Jehlicka, J.; Munshi, T. FT-Raman Spectroscopic Study of Calcium-Rich and Magnesium-Rich Carbonate Minerals. Spectrochim. Acta A 2005, 61, 2273-2280
23. Böttcher, M.E.; Gehlken, P.-L.; Steele, D.F. Characterization of Inorganic and Biogenic Magnesian Calcites by Fourier Transform Infrared Spectroscopy. Solid State Ionics 1997, 101-103, 1379-1385
24. Cheilakou, E.; Troullinos, M.; Koui, M. Identification of Pigments on Byzantine Wall Paintings from Crete (14th Century AD) Using Non-Invasive Fiber Optics Diffuse Reflectance Spectroscopy (FORS). J. Archaeol. Sci. 2014, 41, 541-555

For TOC only

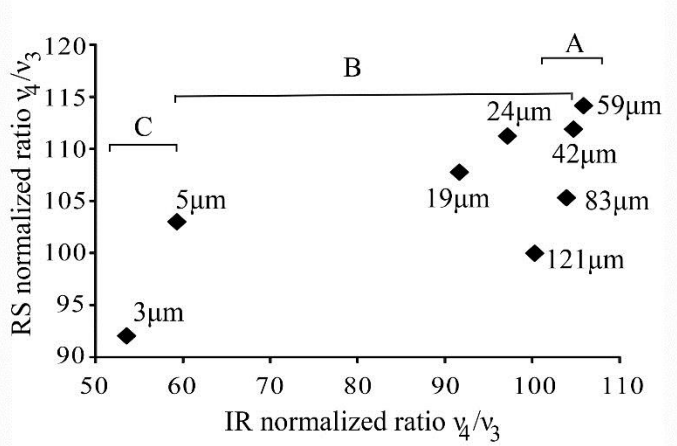
A
B
C
59µm
24µm
42µm
19µm
83µm
5µm
121µm
3µm
120
115
110
105
100
95
90
50
60
70
80
90
100
110
RS normalized ratio ν_4/ν_3
IR normalized ratio ν_4/ν_3